



**Structure-property relations of amphiphilic poly(furfuryl glycidyl ether)-block-poly(ethylene glycol) macromonomers at the air-water interface**

Journal:	<i>Polymer Chemistry</i>
Manuscript ID	PY-ART-05-2020-000697.R1
Article Type:	Paper
Date Submitted by the Author:	16-Jul-2020
Complete List of Authors:	Adatia, Karishma; University of Stuttgart, Institute of Interfacial Process Engineering and Plasma Technology Holm, Alexander; Stanford University, Department of Chemical Engineering Southan, Alexander; University of Stuttgart, Institute of Interfacial Process Engineering and Plasma Technology Frank, Curt; Stanford University, Chemical Engineering Tovar, Günter; University of Stuttgart, Institute of Interfacial Process Engineering and Plasma Technology; Fraunhofer-Institut für Grenzflächen und Bioverfahrenstechnik,

## ARTICLE

## Structure-property relations of amphiphilic poly(furfuryl glycidyl ether)-*block*-poly(ethylene glycol) macromonomers at the air-water interface

Received 00th January 20xx,  
Accepted 00th January 20xx

DOI: 10.1039/x0xx00000x

Karishma K. Adatia,<sup>a,b</sup> Alexander Holm,<sup>b</sup> Alexander Southan,<sup>a\*</sup> Curtis W. Frank,<sup>b\*</sup> and Günter E.M. Tovar<sup>a,c\*</sup>

**Abstract.** To deepen our knowledge of the film formation and the structure-property relations of poly(furfuryl glycidyl ether)-*block*-poly(ethylene glycol) (PFGE<sub>p</sub>-*b*-PEG<sub>q</sub>) macromonomers at the air-water interface, we synthesized PFGE<sub>p</sub>-*b*-PEG<sub>q</sub> in six different block lengths. The molar mass of the PFGE<sub>p</sub>-*b*-PEG<sub>q</sub> macromonomers varied from ~2 000 g mol<sup>-1</sup> to ~7 000 g mol<sup>-1</sup> and included a wide range of hydrophilic-lipophilic balance (HLB) values between 3.6 and 13.9. Surface pressure-area ( $\pi$ -A) isotherms of these amphiphilic macromonomers revealed that the block lengths and the molar mass influence the isotherm shape and onset. Smaller, more hydrophobic macromonomers (HLB < 8) showed a steeper surface pressure increase in the liquid condensed phase compared to larger, more hydrophilic macromonomers with HLB > 8. The molecular area for isotherm onsets increased almost linearly with growing molar mass of the macromonomers. Static and dynamic film stability measurements demonstrated limited stability of all macromonomer monolayers at the air-water interface. The more hydrophilic macromonomers PFGE<sub>8</sub>-*b*-PEG<sub>79</sub>, PFGE<sub>18</sub>-*b*-PEG<sub>66</sub> and PFGE<sub>13</sub>-*b*-PEG<sub>111</sub> (HLB > 8) showed higher film stability compared to the more hydrophobic macromonomers (HLB < 8). Hysteresis experiments displayed an almost linear increase of the film degradation with rising HLB values of the macromonomers. Due to partial film recovery of our macromonomers, we propose an interplay between a reversible folding and an irreversible submersion mechanism for the macromonomer monolayers at the air-water interface. The molecular structure and the film forming ability of the macromonomers at the air-water interface indicate that they are promising surface functionalization reagents for materials formed from aqueous solutions, such as hydrogels. In this regard, PFGE<sub>10</sub>-*b*-PEG<sub>9</sub> is the most promising hydrogel surface functionalization reagent, because it can introduce the highest number of functional groups per surface area.

### Introduction

The Langmuir film balance technique is a highly valuable method for the preparation and characterization of monolayers formed by amphiphilic molecules at the air-water interface.<sup>1-5</sup>

In the last 100 years it has been applied to a broad range of substances such as small molecules,<sup>6-8</sup> polymers,<sup>9,10</sup> particles,<sup>11</sup> metal complexes<sup>12, 13</sup> and supra-molecular assemblies<sup>14, 15</sup> to explore monolayer formation, molecular area per amphiphile, interfacial organization and film stability.<sup>2</sup>

In particular, amphiphilic macromolecules based on poly(ethylene glycol) (PEG)<sup>16-20</sup> such as PEG-based poly(benzyl ether)

monodendrons,<sup>21</sup> poly(ethylene glycol)-*block*-polystyrene (PEG-*b*-PS)<sup>9, 22, 23</sup> and PEGylated-lipomers<sup>24</sup> have been intensively investigated to broaden knowledge of their molecular features at the air-water interface. Kampf *et al.* for example demonstrated that the molecular area of PEG-based poly(benzyl ether) monodendrons grew linearly with the molar mass and that a longer hydrophilic tail improved the film stability.<sup>21</sup> Furthermore, PEG-containing macromolecules often display conformational changes from pancake-like to mushroom-like to brush-like structures during monolayer compression.<sup>24</sup> However, this model is not applicable to all PEG-containing polymers, as shown by Faure *et al.* for PEG-*b*-PS block copolymers.<sup>9</sup> This indicates that the surface characteristics of PEG-based macromolecules are diverse, and each molecular composition may need individual exploration.

In the case of poly(furfuryl glycidyl ether)-*block*-poly(ethylene glycol) macromonomers (PFGE<sub>p</sub>-*b*-PEG<sub>q</sub>), there is almost no knowledge available regarding their behavior at the air-water interface. In fact, only the micelle formation in water of poly(furfuryl glycidyl ether)-*block*-poly(ethylene glycol) block copolymers and the critical micelle concentration of PFGE<sub>p</sub>-*b*-PEG<sub>q</sub> macromonomers has been reported.<sup>25, 26</sup> In previous work, we used PFGE<sub>p</sub>-*b*-PEG<sub>q</sub> macromonomers for hydrogel functionalization with multiple,

<sup>a</sup> Institute of Interfacial Process Engineering and Plasma Technology IGVP, University of Stuttgart, Nobelstr.12, D-70569 Stuttgart, Germany.

<sup>b</sup> Department of Chemical Engineering, Stanford University, Stanford, CA 94305, USA.

<sup>c</sup> Fraunhofer Institute for Interfacial Engineering and Biotechnology IGB, Nobelstr. 12, D-70569 Stuttgart, Germany.

\* Corresponding authors: guenter.tovar@igvp.uni-stuttgart.de, cwfrank@stanford.edu, alexander.southan@igvp.uni-stuttgart.de.

Electronic Supplementary Information (ESI) available: [details of any supplementary information available should be included here]. See DOI: 10.1039/x0xx00000x

clickable anchor points. The terminal 4-vinyl benzyl moiety of the macromonomer was utilized as a polymerizable unit for the covalent immobilization of the macromonomer in the hydrogel bulk and the furan side chains served as molecular anchor points for post-synthetic Diels-Alder reactions.<sup>26</sup> To explore whether PFGE<sub>p</sub>-*b*-PEG<sub>q</sub> macromonomers are not only able to functionalize the hydrogel bulk, but also could self-assemble to form monolayers at the surface of aqueous solutions and thus result in hydrogel surface functionalization after curing, further knowledge about the film forming properties and the monolayer stability is needed. Surface functionalized hydrogels are especially attractive for tissue engineering,<sup>27</sup> drug delivery<sup>28, 29</sup> and biochemical<sup>30, 31</sup> applications.

Therefore, PFGE<sub>p</sub>-*b*-PEG<sub>q</sub> macromonomers with different average molar masses and block ratios were synthesized and characterized with the Langmuir film balance technique. This will contribute to a deeper understanding of the structure-property relations of PFGE<sub>p</sub>-*b*-PEG<sub>q</sub> macromonomers at the air-water interface and facilitate an evaluation of PFGE<sub>p</sub>-*b*-PEG<sub>q</sub> macromonomers as potential hydrogel surface functionalization reagents.

## Experimental Section

**Materials.** Potassium (98%), 4-vinyl benzyl chloride (4VBC) (90%), and calcium hydride (95%), were purchased from Sigma Aldrich (Darmstadt, Germany) and ethylene oxide (EO) from the Linde group (Dublin, Ireland). Diphenylmethane (DPM) (99%), silica gel 60 with a particle size of 0.063 mm – 0.200 mm and active basic aluminium oxide 66 with a particle size of 0.063 mm – 0.200 mm were bought from Merck KGaA (Darmstadt, Germany). Furfuryl glycidyl ether (FGE) was obtained from Acros organics (Geel, Belgium) and purified by column chromatography (silica gel, solvent gradient from EtOAc : PE = 1 : 1 to EtOAc : PE = 3 : 1). Tetrahydrofuran (THF), isopropanol (*i*PrOH), ethanol (EtOH), methanol (MeOH), chloroform (CHCl<sub>3</sub>) and diethylether were purchased in HPLC grade from VWR chemicals (Radnor, USA) and ethyl acetate (EtOAc) was obtained from J.T. Baker (Phillipsburg, USA). For the macromonomer synthesis, THF was dried at least 2 days over calcium hydride and freshly distilled under argon before use. EO was dried by passing through a column of calcium hydride. 4VBC was flashed over basic aluminium oxide, stirred over calcium hydride for 4 days and distilled under vacuum at 50 °C and 10<sup>-1</sup> mbar. If not further explained, all chemicals were used as received.

**Synthesis.** PFGE<sub>p</sub>-*b*-PEG<sub>q</sub> macromonomers were synthesized *via* anionic polymerization as described previously.<sup>26</sup> Briefly, diphenylmethyl potassium (DPMK) was used as an initiator for the polymerization of FGE. Then EO was added to the living poly(furfuryl glycidyl ether) (PFGE) chains to form the second block. The living chain ends were terminated with 4-vinyl benzyl chloride for vinyl benzyl end groups. For hydroxyl end groups, the termination was performed with methanol. The block lengths were determined *via* <sup>1</sup>H NMR spectroscopy by calculating the ratio between the integral of the initiator protons and the integral of the protons of the respective repeating unit.<sup>26</sup>

<sup>1</sup>H NMR (500 MHz, CDCl<sub>3</sub>): δ [ppm] = 3.22 – 3.72 (m, 150, *a, b, c, h, i*), 4.13 (m, 1 H, *o*), 4.42 – 4.45 (m, 20, *d*), 4.55 (s, 2 H, *j*), 5.22 – 5.24 (m, 1 H, *n*), 5.72 – 5.75 (m, 1 H, *n*), 6.26 – 6.30 (m, 20, *e, f*), 6.69 – 7.13 (m, 1 H, *m*), 7.12 -7.24 (m, 10 H, *p*), 7.29 -7.30 (m, 4 H, *k*), 7.34 – 7.39 (m, 10 H, *g*). The alphabetical proton assignments refer to Figure SI 1 - 4.

**Polymer characterization.** <sup>1</sup>H NMR spectra were recorded on an “Avance 500” (500 MHz) spectrometer from Bruker (Billierica, USA). Chloroform-*d*<sub>1</sub> was used as solvent and tetramethylsilane as internal standard. For size exclusion chromatography (SEC) the macromonomers were dissolved in THF for 24 h through a 0.2 μm poly(tetrafluoro ethylene) syringe filter before injecting 50 μL of the sample into a “SECURITY System” from PSS GmbH (Darmstadt, Germany). The system had a PSS SDV precolumn (8 mm x 50 mm), two PSS SDV 1000 Å (8 mm x 300 mm) columns and a refractive index (RI) detector. THF (HPLC grade) was used as solvent, the flow rate was 0.5 mL min<sup>-1</sup> and the columns were calibrated with polystyrene standards “ReadyCal” from PSS GmbH (Darmstadt, Germany). For the analysis of the measurements PSS WinGPC Unichrom software version 8.10 was used.

**Langmuir film balance experiments.** For Langmuir film balance experiments a KSV-5 000 Nima Langmuir-Blodgett trough with the dimensions 150 mm x 580 mm from Biolin Scientific Holding AB (Stockholm, Sweden) with two movable barriers was used. Before each experiment the barriers and the trough were cleaned carefully with a soft brush and then rinsed three times with deionized (DI) water, ethanol and finally again with DI water. About 1 300 mL ultrapure MilliQ water from a Millipore system was used as subphase. After an equilibration time of 30 minutes to 21.7 °C (± 0.2 °C), the barriers were compressed with a constant speed of 50 mm min<sup>-1</sup> to a trough area *A*<sub>t</sub> of 100 cm<sup>2</sup> so that the surface could be cleaned by aspirating 50 mL from the surface. Then the barriers were expanded to the maximum *A*<sub>t</sub> and few microliters of a 1 mg mL<sup>-1</sup> macromonomer solution in CHCl<sub>3</sub> (HPLC grade) were spread carefully on the surface using a microsyringe. The compression for the film isotherm experiments started at a *A*<sub>t</sub> of 780 cm<sup>2</sup> and ended at 100 cm<sup>2</sup>. The amounts of the macromonomers were chosen in such a way that the isotherm onset appeared around 700 cm<sup>2</sup> (± 50 cm<sup>2</sup>) trough area. The exact amount of block polymer used in each experiment is given in the supporting information (Table SI 1). All glassware for the preparation of the macromonomer solutions were cleaned in a base bath containing 8 L *i*PrOH, 2 L DI water and 500 g potassium hydroxide and rinsed numerous times with DI and MilliQ water before it was dried in the oven at 120 °C. After a waiting period of 20 minutes for solvent evaporation, all experiments were performed with a constant barrier speed of both barriers of 10 mm min<sup>-1</sup> (0.5 cm<sup>2</sup> s<sup>-1</sup>), both in compression as well as expansion.  $\pi$  is defined as the difference between the surface tension  $\gamma_0$  of pure water and the surface tension  $\gamma$  of water with surfactant:

$$\pi = \gamma_0 - \gamma \quad (1)$$

$\pi$  was measured using a rinsed Wilhelmy plate connected to a highly sensitive film balance. The Wilhelmy plate method has an

experimental error of approximately  $0.1 \text{ mN m}^{-1}$ .<sup>21, 26</sup> For the hysteresis and recovery experiments, the barriers were immediately expanded to the maximum trough area after compression. The isotherm onset was defined at  $\pi = 0.3 \text{ mN m}^{-1}$  where the measured value could clearly be distinguished from measurement noise. In the film stability experiments, the macromonomer film was compressed to a starting surface pressure  $\pi_0 = 5 \text{ mN m}^{-1}$  and then the barriers stayed at that position for 1 h so that the surface pressure drop ( $\Delta\pi$ ) could be measured.

**Characteristic polymer values.** In addition to their molar masses and molar mass dispersities, polymers were categorized by their hydrophilic-lipophilic balance (HLB) value:<sup>26, 32, 33</sup>

$$HLB = 20 \cdot \left(1 - \frac{M_l}{M_n}\right) \quad (2)$$

The molecular structure of the PFGE<sub>p</sub>-*b*-PEG<sub>q</sub> macromonomers is shown in Figure 1 and the HLB values were calculated by using the molar mass of the lipophilic moiety ( $M_l$ ) and the molar mass of the macromonomers ( $M_n$ ), which were both determined by NMR (Table 1). In particular, the lipophilic part of the macromonomers comprises the PFGE-block and the 4-vinyl benzyl end group, whereas the hydrophilic part is given by the PEG-block (Figure 1, Table 1).

Furthermore, the amount surface coverage factor  $\theta_n$  and the mass surface coverage factor  $\theta_m$  were calculated according to equation 3 and 4 to quantify how much polymer per area are needed to cause the onset surface pressure of  $\pi = 0.3 \text{ mN m}^{-1}$ .

$$\theta_n = \frac{n}{a_0} \quad (3)$$

$$\theta_m = \frac{n \cdot M_n}{a_0} = \theta_n \cdot M_n \quad (4)$$

Here,  $n$  is the amount of macromonomers used in the specific experiment and  $a_0$  is the trough area at the isotherm onset. Derived from  $\theta_n$  the surface functionality factor  $S$  can be calculated by multiplication with  $p$ , which is the number of repeating units of the PFGE-block.

$$S = \frac{n \cdot p}{a_0} = \theta_n \cdot p \quad (5)$$

In theory, each FGE repeating unit exhibits a furan moiety, which is available for post-synthetic modifications.<sup>26</sup> In contrast to the surface coverage factor  $\theta_n$ , the surface functionalization factor  $S$  expresses how many functional furan groups per area are available through our macromonomers.

Furthermore, the recovery of the macromonomers to the air-water interface after five hysteresis cycles was measured by the surface pressure difference ( $\Delta\pi$ ) between the hysteresis maximum of the recovery cycle ( $\pi_{\text{HM},r}$ ) and the hysteresis maximum of the fifth hysteresis cycle ( $\pi_{\text{HM},5}$ ) (equation 6). For normalized values the

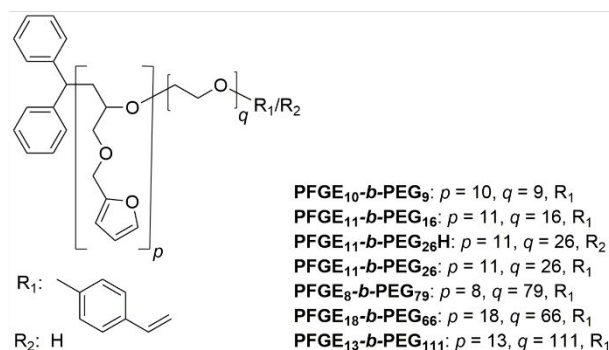
surface pressure of the hysteresis maximum of the first hysteresis cycle ( $\pi_{\text{HM},1}$ ) was set to 100%.

$$\Delta\pi = \pi_{\text{HM},r} - \pi_{\text{HM},5} \quad (6)$$

**Statistical data evaluation.** The statistical analysis was performed by one-way analysis of variance (ANOVA) using the Holm-Bonferroni post-hoc test with the software OriginPro 9.1 from OriginLab Corporation (Northampton, USA). An effect was judged significant when the differences between individual mean values were significant with  $p < 0.05$ .

## Results and Discussion

**a**



**b**

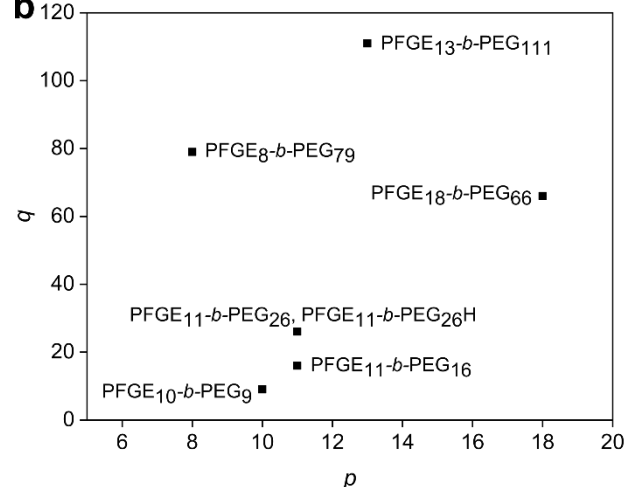


**Figure 1:** a) Molecular structure and b) matrix depiction of  $\alpha$ -diphenylmethyl- $\omega$ -4-vinyl benzyl-poly(furfuryl glycidyl ether)-*block*-poly(ethylene glycol) (PFGE<sub>p</sub>-*b*-PEG<sub>q</sub>) macromonomers.  $p$  is the number of repeating units in the PFGE-block and  $q$  is the number of repeating units in the (PEG)-block of the respective macromonomer.

**Macromonomer synthesis.** The aim of this work is to deepen the knowledge of film formation and structure-property relations of poly(furfuryl glycidyl ether)-*block*-poly(ethylene glycol) macromonomers at the air-water interface and to evaluate them as potential hydrogel surface functionalization reagents. Therefore, we synthesized six different  $\alpha$ -diphenylmethyl- $\omega$ -4-vinyl benzyl-poly(furfuryl glycidyl ether)-*block*-poly(ethylene glycol) macromonomers, which are abbreviated with PFGE<sub>p</sub>-*b*-PEG<sub>q</sub>,

whereby  $p$  is the number of repeating units in the PFGE-block and  $q$  is the number of repeating units in the poly(ethylene glycol) (PEG)-block (Figure 1). The PFGE-block lengths varied from  $p = 8 - 18$  and the PEG-block contained 9 to 111 repeating units. This led to number average molar masses  $M_{n,NMR}$  from 2 220 g mol<sup>-1</sup> to 7 180 g mol<sup>-1</sup> and a broad range of hydrophilic-lipophilic balance (HLB) values between 3.6 and 13.9 (Table 1). Furthermore, the macromonomer PFGE<sub>11</sub>-*b*-PEG<sub>26</sub> was synthesized with a hydrophobic 4-vinyl benzyl end group (like all the other macromonomers) and with a hydrophilic hydroxy end group (PFGE<sub>11</sub>-*b*-PEG<sub>26</sub>H) to explore the influence of the end group at the air-water interface. The molecular structures and a matrix depiction of all macromonomers are shown in Figure 1. Additionally, the number average molar masses and the HLB values are summarized in Table 1.

**Table 1:** Overview of number average molar mass ( $M_n$ ), average molar mass of the lipophilic polymer moiety ( $M_l$ ), average molar mass of the hydrophilic polymer moiety ( $M_h$ ), weight average molar mass ( $M_w$ ), molar mass dispersity ( $\mathcal{D}_{SEC}$ ) and hydrophilic-lipophilic balance (HLB) values of macromonomers used in this study. The molar masses and molar mass dispersities were determined by nuclear magnetic resonance spectroscopy (NMR) or size exclusion chromatography (SEC), which is indicated by the subscript.

sample	$M_{n,NMR}$ [g mol <sup>-1</sup> ]	$M_{l,NMR}$ [g mol <sup>-1</sup> ]	$M_{h,NMR}$ [g mol <sup>-1</sup> ]	$M_{n,SEC}$ [g mol <sup>-1</sup> ]	$M_{w,SEC}$ [g mol <sup>-1</sup> ]	$\mathcal{D}_{SEC}$	HLB
PFGE <sub>10</sub> - <i>b</i> -PEG <sub>9</sub>	2 220	1 830	400	4 530	4 950	1.09	3.6
PFGE <sub>11</sub> - <i>b</i> -PEG <sub>16</sub>	2 690	1 980	710	2 650	2 960	1.12	5.2
PFGE <sub>11</sub> - <i>b</i> -PEG <sub>26</sub> H	3 010	1 870	1 150	3 000	3 260	1.09	7.6
PFGE <sub>11</sub> - <i>b</i> -PEG <sub>26</sub>	3 130	1 980	1 150	3 140	3 390	1.08	7.3
PFGE <sub>8</sub> - <i>b</i> -PEG <sub>79</sub>	5 000	1 520	3 480	5 020	5 260	1.05	13.9
PFGE <sub>18</sub> - <i>b</i> -PEG <sub>66</sub>	5 970	3 060	2 910	5 190	5 440	1.05	9.7
PFGE <sub>13</sub> - <i>b</i> -PEG <sub>111</sub>	7 180	2 290	4 890	6 660	7 250	1.09	13.6

<sup>1</sup>H NMR spectra (Figure SI 1 - 4) confirmed the successful synthesis of all macromonomers described in Figure 1, since the proton signals are in accordance with the literature. Additionally, SEC traces showed narrow, monomodal molar mass distributions with low molar mass dispersities (Figure SI 5). Overall, the molar masses determined by <sup>1</sup>H NMR ( $M_{n,NMR}$ ) and SEC ( $M_{n,SEC}$ ) in Table 1 were in good agreement. All macromonomers from Table 1 showed good solubility in organic solvents like THF, CHCl<sub>3</sub> and MeOH. In addition, the three previously published macromonomers PFGE<sub>8</sub>-*b*-PEG<sub>79</sub>, PFGE<sub>18</sub>-*b*-PEG<sub>66</sub> and PFGE<sub>13</sub>-*b*-PEG<sub>111</sub> were soluble in water because of their comparatively long PEG-block.<sup>26, 34, 35</sup>

## ARTICLE

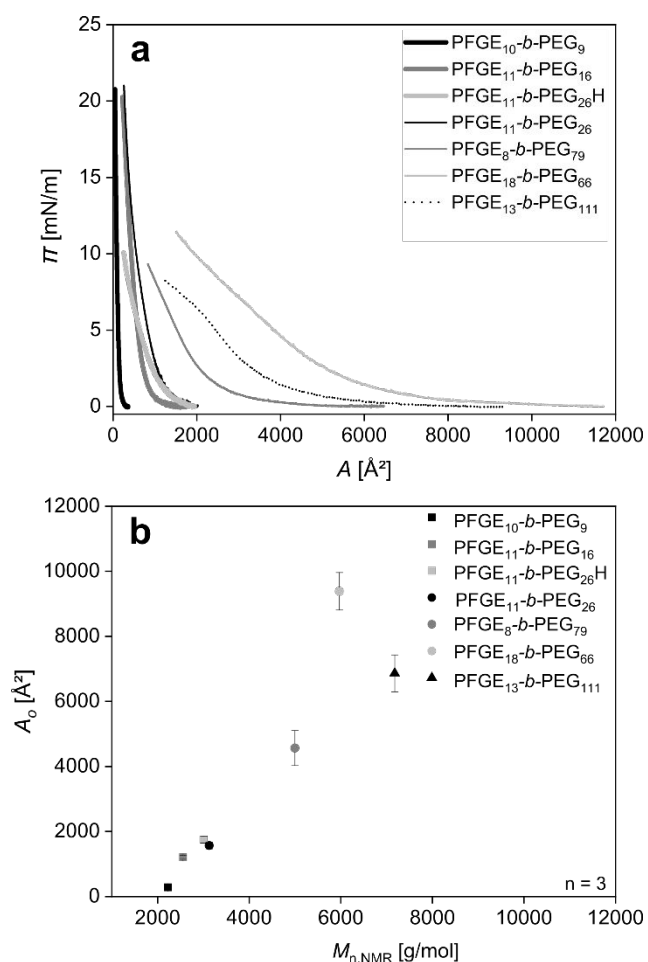


**Figure 2:** a) Surface pressure-area ( $\pi$ - $A$ ) isotherms and b) correlation of the area per molecule at the onset ( $A_0$ ) with the molar mass ( $M_{n,NMR}$ ) of the macromonomers from Table 1.  $A_0$  was defined at  $\pi = 0.3 \text{ mN m}^{-1}$ . The error bars (given in parentheses) indicating the standard deviation are roughly the same size as the symbols for the rather hydrophobic macromonomers PFGE<sub>10</sub>-b-PEG<sub>9</sub> (31  $\text{\AA}^2$ ), PFGE<sub>11</sub>-b-PEG<sub>16</sub> (55  $\text{\AA}^2$ ), PFGE<sub>11</sub>-b-PEG<sub>26</sub>H (109  $\text{\AA}^2$ ) and PFGE<sub>11</sub>-b-PEG<sub>26</sub> (99  $\text{\AA}^2$ ).

**$\pi$ - $A$  Isotherms.** Film formation at the air-water interface of all macromonomers from Table 1 was assessed by the Langmuir technique. The good reproducibility of our  $\pi$ - $A$  isotherm experiments, especially for PFGE<sub>11</sub>-b-PEG<sub>16</sub>, is shown in Figure SI 6. Furthermore, the  $\pi$ - $A$  isotherm onsets did not significantly change upon varying the barrier speed in the range of  $10 \text{ mm min}^{-1}$  to  $50 \text{ mm min}^{-1}$  (Figure SI 7 and Figure SI 8), which is in line with  $\pi$ - $A$  isotherms of other amphiphiles like ytterbium bisphthalocyanine or arachidic acid.<sup>36, 37</sup> We chose a barrier speed of  $10 \text{ mm min}^{-1}$  for our further experiments, which is frequently used in the literature, to give the system as much time as possible to equilibrate and to avoid kinetic effects.<sup>21, 36-38</sup>

As shown in Figure 2a, all macromonomers caused an increase of surface pressure ( $\pi$ ) when compressed to smaller areas per molecule ( $A$ ), which demonstrates that the macromonomers were present at the air-water interface. This is a clear proof of their surface activity, which is in accordance with previous surface activity measurements *via* bubble pressure tensiometry of the water-soluble macromonomers PFGE<sub>8</sub>-b-PEG<sub>79</sub>, PFGE<sub>18</sub>-b-PEG<sub>66</sub> and PFGE<sub>13</sub>-b-PEG<sub>111</sub>. The tensiometry measurements revealed  $\pi$  up to  $18 \text{ mN m}^{-1}$  for PFGE<sub>13</sub>-b-PEG<sub>111</sub>,  $19 \text{ mN m}^{-1}$  for PFGE<sub>18</sub>-b-PEG<sub>66</sub> and  $21 \text{ mN m}^{-1}$  for PFGE<sub>8</sub>-b-PEG<sub>79</sub> when the polymer concentration was increased above the critical micelle concentration of roughly  $0.3 \text{ mg mL}^{-1}$ .<sup>26</sup>

$\pi$ - $A$  isotherms (Figure 2a) of the macromonomers (Figure 1a and Table 1) revealed the influence of block lengths and molar masses on the isotherm shape and onset. All macromonomers started in the gas phase with a low  $\pi$  and transferred into the liquid-expanded state with a steeper slope during compression. The larger the amphiphile, the more the course of the  $\pi$ - $A$  isotherm was shifted to larger areas per molecule  $A$ . This is in line with Kampf *et al.*, who reported a  $\pi$ - $A$  isotherm shift to a growing  $A$  with increasing monodendron size.<sup>21</sup> Moreover, the smaller, more hydrophobic macromonomers (HLB < 8) showed a steeper ascent in the liquid condensed phase compared to larger, more hydrophilic macromonomers with HLB > 8. A similar trend was described for PEG-based monodendrons with growing PEG-tails.<sup>21</sup>

The change in slope of the  $\pi$ - $A$  isotherm for the macromonomer PFGE<sub>13</sub>-b-PEG<sub>111</sub> around  $6 \text{ mN m}^{-1}$  may suggest a transition from pancake-like structure to a mushroom-like or brush-like structure of the PEG chains at the water air interface, as observed by Yang *et al.* for fluoroalkyl-terminated PEGs.<sup>39</sup> Similar transitions of PEG-based polymers were also reported by Fauré *et al.*, Baekmark *et al.* and Wiesenthal *et al.*<sup>9, 24, 40</sup> We did not observe a transition state for the other macromonomers, presumably due to the shorter PEG-chains, which is in line with Clop *et al.* who explained that a certain chain length is necessary for a transition state to occur.<sup>41</sup>

We further investigated the structure-property relations of the macromonomers at the air-water interface and found that the area per molecule at the isotherm onset ( $A_0$ ) correlates with the number

average molar mass  $M_{n,NMR}$  of the macromonomers (Figure 2b). Hereby,  $M_{n,NMR}$  of our macromonomers were between 2 220 g mol<sup>-1</sup> and 7 180 g mol<sup>-1</sup> and the measured  $A_0$  varied between 279 Å<sup>2</sup> and 9 386 Å<sup>2</sup>. Figure 2b shows that an increase of  $M_{n,NMR}$  correlates in an almost linear way with  $A_0$ , whereby the mean values of  $A_0$  differ significantly from each other with  $p < 0.01$ . Except for PFGE<sub>18</sub>-*b*-PEG<sub>66</sub>, the higher the  $M_{n,NMR}$  of the macromonomer, the more area each polymer occupies at the air-water interface. A similar trend was also published by Clop *et al.* for PEG-grafted dipalmitoyl phosphatidylethanolamines, in which  $A_0$  increased from 660 Å<sup>2</sup> to 6 000 Å<sup>2</sup> when the molar mass of the PEG-block grew from 350 g mol<sup>-1</sup> to 5 000 g mol<sup>-1</sup>.<sup>41</sup> Also Kampf *et al.* observed a linear correlation of the molar mass with the molecular area of their monodendrons at the air-water interface.<sup>21</sup>

Moreover, we examined whether the hydrophobic 4-vinyl benzyl unit at the end of the hydrophilic PEG-block has an influence on the surface coverage at the air-water interface. Therefore, we synthesized two analogous block copolymers PFGE<sub>11</sub>-*b*-PEG<sub>26</sub> and PFGE<sub>11</sub>-*b*-PEG<sub>26</sub>H, which only differ in their end group (Figure 1). PFGE<sub>11</sub>-*b*-PEG<sub>26</sub> was terminated with a hydrophobic 4-vinyl benzyl end group (like all of our other macromonomers) and PFGE<sub>11</sub>-*b*-PEG<sub>26</sub>H ends with a hydrophilic hydroxyl moiety. According to equation 3, PFGE<sub>11</sub>-*b*-PEG<sub>26</sub> shows a higher amount surface coverage factor  $\Theta_n$  with 25 pmol cm<sup>-2</sup> ± 7 pmol cm<sup>-2</sup> compared to PFGE<sub>11</sub>-*b*-PEG<sub>26</sub>H with  $\Theta_n = 22$  pmol cm<sup>-2</sup> ± 4 pmol cm<sup>-2</sup> (Table SI 2). The mass surface coverage factor  $\Theta_m$  from equation 4 is also higher for PFGE<sub>11</sub>-*b*-PEG<sub>26</sub> with  $\Theta_m = 79$  ng cm<sup>-2</sup> ± 22 ng cm<sup>-2</sup> than for PFGE<sub>11</sub>-*b*-PEG<sub>26</sub>H with  $\Theta_m = 65$  ng cm<sup>-2</sup> ± 1 ng cm<sup>-2</sup> (Table SI 2). Though we measured small differences of  $\Theta_n$  and  $\Theta_m$  between the two differently terminated polymers, these differences are not significant with  $p > 0.05$ . Kyeremateng *et al.* in contrast described a change in the surface activity resulting from perfluorination of the end group of their poly(propylene)-*block*-poly(isopropylidene glycerol methacrylate) block copolymer, but did not mention the significance.<sup>42</sup> They explained that the increase in hydrophobicity resulted in a different allocation of their polymer at the surface.<sup>42</sup> In fact, the new fluoro-end group with  $M_{n,NMR} = 600$  g mol<sup>-1</sup> increased the molar mass of the poly(propylene) block with  $M_{n,NMR} = 1 570$  g mol<sup>-1</sup> up to 38 %, whereas our 4-vinyl benzyl end group ( $M_{n,NMR} = 117$  g mol<sup>-1</sup>) caused a weight increase of only 10 % of the PEG-block ( $M_{n,NMR} = 1 150$  g mol<sup>-1</sup>). Hence, we conclude that the relatively small structural change through the end group of our macromonomer caused very little differences in the conformation at the air-water interface and therefore did not influence the surface coverage significantly. This is advantageous for the synthesis, because the implementation of a more polar polymerizable unit in form of an acryloyl moiety led to auto polymerization.<sup>26</sup>

Overall, the  $\pi$ - $A$  isotherms revealed that all macromonomers are able to localize at the air-water interface and show film formation, which is a fundamental prerequisite for the application as surface-functionalization reagent for materials prepared from aqueous solution such as hydrogels. Compared to the end group, the molar mass of the macromonomers have a much stronger influence on the surface properties like the isotherm shape and onset. In fact, we observed an almost linear growth of the isotherm onsets with growing molar mass of the macromonomers.

**Film stability.** Since we found that all PFGE<sub>*p*</sub>-*b*-PEG<sub>*q*</sub> macromonomers are able to form Langmuir monolayers at the air-water interface, we were interested in the film stability under static and dynamic conditions. For static investigations we used a very similar approach to Deschênes *et al.*, as we monitored the  $\pi$  over time ( $t$ ) at a starting surface pressure ( $\pi_0$ ) of 5 mN m<sup>-1</sup> and then kept the trough barriers at a constant area ( $A_c$ ).<sup>43</sup>

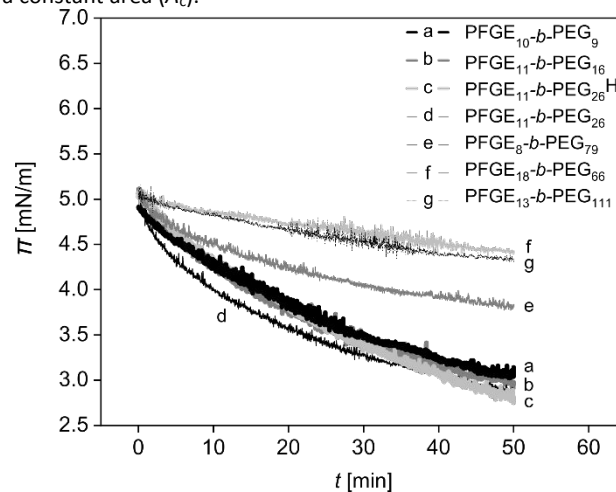


**Figure 3:** Film stability of the macromonomer films from Table 1 determined by measuring the surface pressure ( $\pi$ ) over time ( $t$ ) at constant trough area ( $A_c$ ) with a starting surface pressure ( $\pi_0$ ) of 5 mN m<sup>-1</sup>.

Figure 3 shows that the  $\pi$  of all macromonomer films dropped over time and the jagged lines indicate a dynamic process at the air-water interface.<sup>44</sup> Since  $\pi$  is defined in equation 1 as the difference between the surface tension of water ( $\gamma_0$ ) and the surface tension of water with surfactant ( $\gamma$ ), a surface pressure drop ( $\Delta\pi_d$ ) indicates a decreasing amount of macromonomers at the surface.<sup>45</sup>

During 50 minutes, we observed a surface pressure drop  $\Delta\pi_d$  for the more hydrophilic macromonomers PFGE<sub>8</sub>-*b*-PEG<sub>79</sub>, PFGE<sub>18</sub>-*b*-PEG<sub>66</sub> and PFGE<sub>13</sub>-*b*-PEG<sub>111</sub> between 0.5 mN m<sup>-1</sup> and 1.25 mN m<sup>-1</sup> and a  $\Delta\pi_d$  for the more hydrophobic macromonomers PFGE<sub>10</sub>-*b*-PEG<sub>9</sub>, PFGE<sub>11</sub>-*b*-PEG<sub>16</sub>, PFGE<sub>11</sub>-*b*-PEG<sub>26</sub>H and PFGE<sub>11</sub>-*b*-PEG<sub>26</sub> between 1.8 mN m<sup>-1</sup> and 2.2 mN m<sup>-1</sup> (Figure 3 and Figure SI 9). This demonstrates that the hydrophilic macromonomer films with HLB values > 8, are more stable compared to the hydrophobic films with HLB values < 8. We attribute this to the anchoring effect of the PEG-block at the air-water interface, which was analyzed previously by Kampf *et al.*<sup>21</sup>

To explain the surface pressure decrease over time, there are two possibilities in the literature how amphiphiles can leave a film at the air-water interface: Either they immerse to the subphase, or the molecules transfer from a two dimensional (2D) film to a three dimensional (3D) formation.<sup>46, 47</sup> Both options seem reasonable for our macromonomers. Regarding the first, a submersion was observed for many PEG-based polymers before and PFGE-*b*-PEG block copolymers are additionally known to form micelles in the subphase.<sup>25, 46</sup> Regarding the latter, it is likely that the asymmetric nature of our macromonomers induce monolayer bending which leads to a 2D-3D transition as it was described for multiple amphiphiles.<sup>48-53</sup> Therefore, we believe that a combination of both mechanisms is likely.

We furthermore investigated the monolayer stability under dynamic conditions, for which we measured five hysteresis cycles of each macromonomer (Figure SI 10). For all macromonomers the

surface pressures of the hysteresis maxima ( $\pi_{HM}$ ) decreased with ongoing hysteresis cycles. Moreover, the hysteresis loops, which display the difference between compression and expansion cycle, shrank with increasing number of cycles. This indicates that the system was approaching an equilibrium state. There are different processes in the literature that explain hysteresis loops of a monolayer:<sup>54</sup> I) the Marangoni effect, which describes mass transfer along the interface of two fluids due to a gradient of the surface tension;<sup>55</sup> II) conformation and relaxation processes in the monolayer; III) a collapse of the monolayer into a 3D phase and IV) interchange of molecules between the soluble monolayer and the subphase. We think that our hysteresis loops are most probably a result of an interplay of all these four points. Concerning point I, our macromonomers are exposed to the Marangoni effect, since the movable barriers, which have a different deformation effect on the subphase compared to the film, lead to a surface pressure gradient.<sup>54</sup> Regarding point II and III it was described that folded regions can coexist with the 2D monolayer, whereby further compression changes the fraction of the monolayer in the folds relative to the 2D regions.<sup>48, 56</sup> Such an ongoing 3D fold formation of our macromonomers could explain the successive surface pressure decrease per hysteresis cycle. Additionally, an equilibrium between our macromonomers at the interface and macromonomer micelles is very likely based on the ability of PFGE-*b*-PEG block copolymers to form micelles (point IV).<sup>25</sup>

To quantify the surface pressure decrease during the hysteresis experiment, we fitted the surface pressures of the hysteresis maxima  $\pi_{HM}$  per cycle and looked at the absolute value of the slope ( $s_{HM}$ ). An overview of the linear fits and the coefficients of determination ( $R^2$ ) are given in Figure SI 11 and Table SI 3. If  $s_{HM}$  is big, it indicates a high hysteresis decline, which means more molecules left the air-water interface during each compression-expansion cycle. The mean values of  $s_{HM}$  reach from 1.0 to 4.0 and differ significantly from each other with  $p < 0.01$ . In Figure 4a, the correlation of the surface pressure decline and the HLB value is presented. It shows that with rising HLB values of the macromonomer,  $s_{HM}$  decreases. For example, the most hydrophobic macromonomer PFGE<sub>10</sub>-*b*-PEG<sub>9</sub> has the steepest slope ( $s_{HM} = 3.7$ ) and the most hydrophilic macromonomer PFGE<sub>8</sub>-*b*-PEG<sub>79</sub> shows the lowest slope ( $s_{HM} = 1.4$ ). Furthermore, the surface pressure of the more hydrophobic macromonomer films of PFGE<sub>10</sub>-*b*-PEG<sub>9</sub>, PFGE<sub>11</sub>-*b*-PEG<sub>16</sub>, PFGE<sub>11</sub>-*b*-PEG<sub>26</sub>H and PFGE<sub>11</sub>-*b*-PEG<sub>26</sub> decreased stronger during the hysteresis experiment compared to the more hydrophilic macromonomers PFGE<sub>18</sub>-*b*-PEG<sub>66</sub>, PFGE<sub>8</sub>-*b*-PEG<sub>79</sub> and PFGE<sub>13</sub>-*b*-PEG<sub>111</sub>. This is in line with the static stability experiments in Figure 3.

Besides that, we exposed the macromonomers to compression and expansion forces for 45 min, 90 min and 225 minutes to investigate the effect of the force exposure time. We kept the number of hysteresis cycles constant at five cycles as we know from the hysteresis experiment that a higher number of hysteresis cycles leads to more decline of the macromonomer films. In Figure SI 7 and Figure SI 8, we showed that the barrier speed has no significant influence on the  $\pi$ - $A$  isotherm of the macromonomers. This enables us to investigate the time dependent hysteresis decline at a constant number of hysteresis cycles by varying the barrier speed from 10 mm min<sup>-1</sup> to 50 mm min<sup>-1</sup>. Five hysteresis cycles at a barrier speed of 50 mm min<sup>-1</sup>, 25 mm min<sup>-1</sup> and 10 mm min<sup>-1</sup> resulted in a force

exposure time of 45 min, 90 min and 225 min. Figure SI 12 shows that the film decline is higher when the macromonomer is exposed to compression and expansion forces for longer time.

In conclusion, all macromonomers showed limited film stability under static and dynamic conditions, whereby the films of the more hydrophobic macromonomers (HLB values < 8) were less stable compared to the films of the more hydrophilic macromonomers (HLB values > 8). This might be critical for the application as hydrogel surface functionalization reagents, but since the film decline is time-dependent, a rapid immobilization of the macromonomers could help to circumvent this obstacle.

**Monolayer recovery and molecular mechanism.** After finding out, that our macromonomers were leaving the 2D monolayer over time, we were curious whether they are able to recover to the air-water interface if they have enough time and space. Therefore, we measured five hysteresis cycles, then expanded the barriers of the Langmuir-Blodgett trough to the maximum trough area  $A_t$  of 780 cm<sup>2</sup> and analyzed the surface pressure  $\pi$  after 12 hours. The hysteresis and recovery cycles of PFGE<sub>8</sub>-*b*-PEG<sub>79</sub> are shown in Figure 4b. The analogous experiments of the other macromonomers are demonstrated in Figure SI 10. As described before, the  $\pi$  of the macromonomer films declined with ongoing hysteresis cycles, but after 12 hours, we could measure higher  $\pi$  during the recovery cycle, which indicates the recovery of macromonomers to the air-water interface.

To quantify the recovery, we normalized the  $\pi_{HM}$  of the first hysteresis cycle to 100 % and calculated the  $\pi$  of the other hysteresis and recovery maxima accordingly (equation 6). For all macromonomers we measured a higher surface pressure of the hysteresis maximum in the recovery cycle ( $\pi_{HM,r}$ ) compared to the surface pressure of the fifth hysteresis cycle ( $\pi_{HM,5}$ ), which is shown in Figure 4c. This is significant with  $p < 0.05$  for PFGE<sub>11</sub>-*b*-PEG<sub>26</sub>H, PFGE<sub>10</sub>-*b*-PEG<sub>9</sub>, PFGE<sub>18</sub>-*b*-PEG<sub>66</sub>, PFGE<sub>8</sub>-*b*-PEG<sub>79</sub> and PFGE<sub>13</sub>-*b*-PEG<sub>111</sub>. PFGE<sub>11</sub>-*b*-PEG<sub>16</sub> and PFGE<sub>11</sub>-*b*-PEG<sub>26</sub> do not exhibit significantly higher  $\pi_{HM,r}$  compared to  $\pi_{HM,5}$ , but still follow the same trend (Figure 4c).

The recovery ability of the macromonomers to the air-water interface after five hysteresis cycles was quantified by the surface pressure difference ( $\Delta\pi$ ) between the hysteresis maximum of the recovery cycle ( $\pi_{HM,r}$ ) and the hysteresis maximum of the fifth hysteresis cycle ( $\pi_{HM,5}$ ) (equation 6). This normalized recovery ability of the studied macromonomers is shown in Figure 4d. The mean values of the  $\Delta\pi$  are between 14 % and 45 % and do not differ significantly with  $p > 0.05$  from each other, which means the surface pressure recovery ability of the macromonomers is indistinguishable from each other. This is probably based on the fact that the macromonomer recovery cannot be attributed to a single factor such as the molar mass or the HLB value, but is rather an interplay of various factors like the molecular structure, the rate of compression and molecule entrapments.<sup>47, 57, 58</sup> This multi-factor dependency of the recovery process also explains the relatively high standard deviations in our recovery experiment (Figure 4d).

The ability of the macromonomers to recover to the air-water interface is a strong indication for a folding mechanism as its reversibility was frequently described in the literature.<sup>57, 59, 60</sup>

Solubilization and multilayer collapse processes in contrast are encountered as irreversible.<sup>48, 58</sup> We rather exclude a mechanism which is mainly based on the collapse to multilayers, as we did not observe a collapse pressure, which is typical for multilayer formations.<sup>39</sup> Additionally a multilayer collapse mostly occurs at very high  $\pi$ , when the amphiphiles are compressed beyond their stability limit.<sup>47</sup> Collapse pressures are often in the range of 50 mN m<sup>-1</sup> to 60 mN m<sup>-1</sup>, such as 50 mN m<sup>-1</sup> for PEG-based azo dyes,<sup>61</sup> around 50 mN m<sup>-1</sup> for  $\beta$ -sheet peptides<sup>62</sup> and 60 mN m<sup>-1</sup> of fatty acid films.<sup>63</sup> In contrast our macromonomers were studied at relatively low  $\pi$  between 0 mN m<sup>-1</sup> and 23 mN m<sup>-1</sup>, which is why we don't think our macromonomers collapsed to multilayers.

Since the declined macromonomers did only recover partly, we suggest an interplay between a folding and a submerge mechanism for our macromonomer films. Basically, the folding mechanism explains the recovery of the macromonomers to the air-water interface and the submerge mechanism, which was also discussed during the stability measurements, clarifies why the macromonomers do not recover quantitatively.

Overall, the recovery experiments played an important role to give further insights into the molecular mechanisms of the studied macromonomer monolayers at the air-water interface.

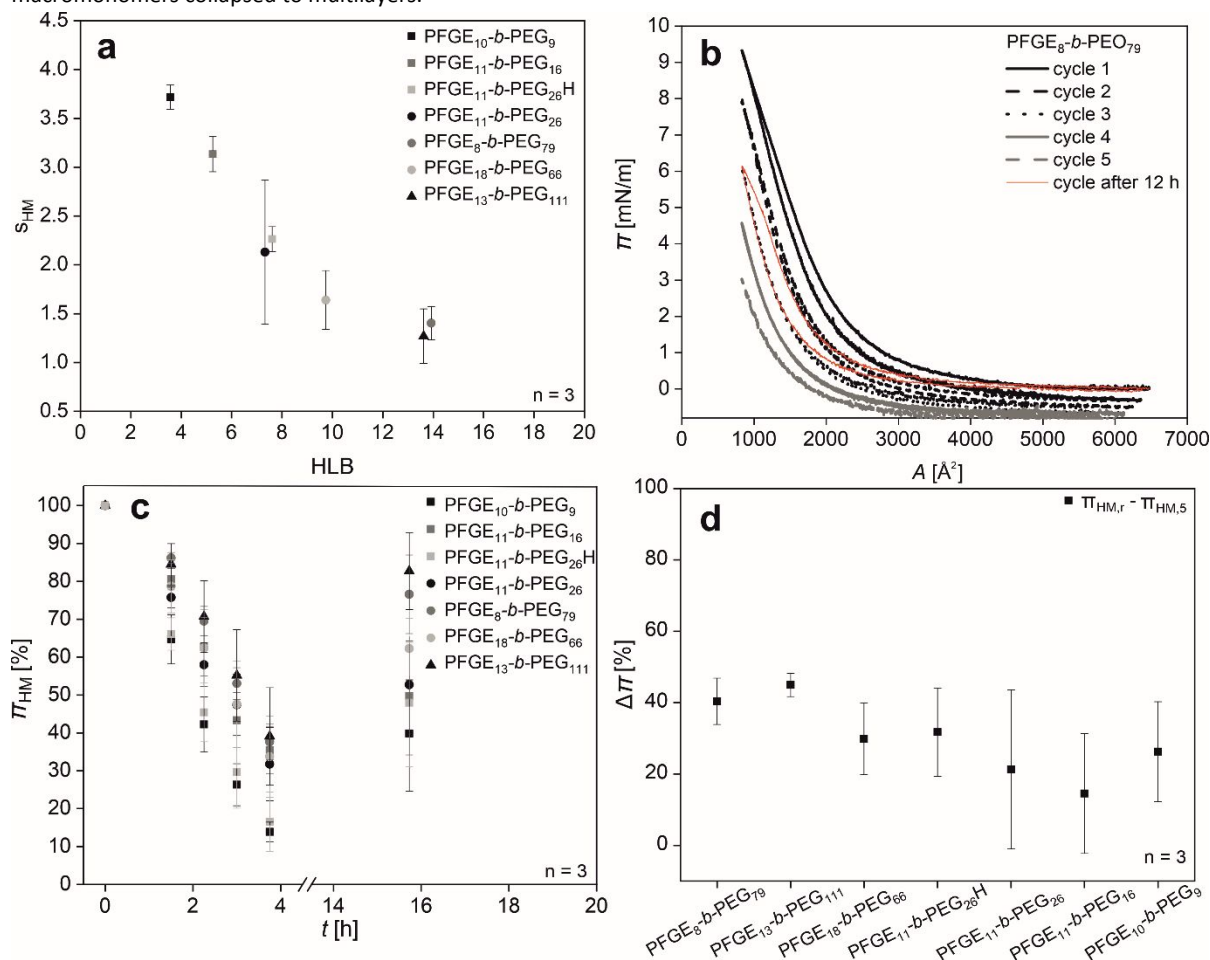


**Figure 4.** a) Correlation of hysteresis decline with the hydrophilic-lipophilic balance (HLB) value of the macromonomers.  $S_{HM}$  is the slope of the linear hysteresis maxima fit from Table SI 3 and represents the hysteresis decline. b) Hysteresis and recovery cycles of PFGE<sub>8</sub>-b-PEG<sub>79</sub>. Analogous hysteresis and recovery cycles of all other macromonomers are given in Figure SI 10. c) Normalized surface pressure of the hysteresis maxima ( $\pi_{HM}$ ) over time ( $t$ ). d) Normalized recovery ability of the studied macromonomers demonstrated by the surface pressure difference ( $\Delta\pi$ ) between the surface pressure of the hysteresis maxima of the recovery cycle ( $\pi_{HM,r}$ ) and the surface pressure of hysteresis maxima of the fifth hysteresis cycle ( $\pi_{HM,5}$ ) (equation 6).

**Evaluation of the macromonomers as potential surface functionalization reagents of hydrogels.** Hydrogel surface functionalization reagents have to fulfill three major criteria: I) they need a functional unit which participates in the material curing reaction for covalent immobilization of the functional groups on the hydrogel surface, II) they should contain functional groups which can serve as molecular anchor points for post-synthetic modifications after the curing reaction and III) they should be able to form stable films at the air-water interface to specifically functionalize the

material surface. The studied macromonomers fully fulfill the first two requirements. The macromonomers contain a polymerizable 4-vinyl benzyl unit for covalent incorporation into radically cross-linkable hydrogels and the furan side chains can react in post-synthetic Diels-Alder reactions.<sup>26</sup> This work shows that all the studied macromonomers were able to form films at the air-water interface, but only with limited stability. Therefore, the third criteria is only partially fulfilled. To overcome this obstacle, we recommend a fast hydrogel curing process for the preparation of surface functionalized

hydrogels. Once the macromonomers are covalently bound to the material, they are immobilized and the film stability becomes irrelevant. Hence, we believe our macromonomers are suitable hydrogel surface functionalization reagents.

To identify which macromonomer is the most favorable hydrogel surface functionalization reagent, we ranked them according to the surface functionalization factor  $S$  (equation 5 and 6).  $S$  quantifies how many functional groups per area are available at the air-water interface. For our macromonomers,  $S$  focuses on the furan groups per area. An overview of the surface functionalization factor and the surface functionality ranking (SFR) of the examined macromonomers are given in Table 2.

According to the surface functionalization factors the hydrophobic macromonomers PFGE<sub>10</sub>-*b*-PEG<sub>9</sub>, PFGE<sub>11</sub>-*b*-PEG<sub>16</sub> and PFGE<sub>11</sub>-*b*-PEG<sub>26</sub> with HLB < 8 are more favorable surface functionalization reagents compared to the hydrophilic macromonomers PFGE<sub>8</sub>-*b*-PEG<sub>79</sub>, PFGE<sub>18</sub>-*b*-PEG<sub>66</sub> and PFGE<sub>13</sub>-*b*-PEG<sub>111</sub> with HLB > 8. The macromonomer PFGE<sub>10</sub>-*b*-PEG<sub>9</sub> is the most promising hydrogel surface functionalization reagent, because it can introduce the highest number of functional groups ( $11.9 \times 10^{-10}$  mol cm<sup>-2</sup>) per surface area (Table 2).

**Table 2:** Surface functionality factor ( $S$ ) and surface functionality ranking (SFR) of the macromonomers used in this study.

sample	$S$ [ $10^{-10}$ mol cm <sup>-2</sup> ]	SFR
PFGE <sub>10</sub> - <i>b</i> -PEG <sub>9</sub>	11.9 ± 1.4	1
PFGE <sub>11</sub> - <i>b</i> -PEG <sub>16</sub>	3.1 ± 0.1	2
PFGE <sub>11</sub> - <i>b</i> -PEG <sub>26</sub>	2.8 ± 0.8	3
PFGE <sub>11</sub> - <i>b</i> -PEG <sub>26</sub> H	2.4 ± 0.4	4
PFGE <sub>13</sub> - <i>b</i> -PEG <sub>111</sub>	0.8 ± 0.1	5
PFGE <sub>18</sub> - <i>b</i> -PEG <sub>66</sub>	0.8 ± 0.1	5
PFGE <sub>8</sub> - <i>b</i> -PEG <sub>79</sub>	0.7 ± 0.1	6

## Conclusions

In summary, we could show the film formation of all six poly(furfuryl glycidyl ether)-*block*-poly(ethylene glycol) (PFGE<sub>p</sub>-*b*-PEG<sub>q</sub>) macromonomers and give more insight into the structure-property relations at the air-water interface by highlighting the influence of the molar mass  $M_{n,NMR}$  and the HLB values on the surface properties.  $\pi$ -A isotherms of the macromonomers revealed that compared to the end group, the molar mass of the macromonomers have a much stronger influence on the surface properties like the isotherm shape and onset. Smaller, more hydrophobic macromonomers (HLB < 8) showed a steeper surface pressure increase in the liquid condensed phase compared to larger, more hydrophilic macromonomers with HLB > 8. Additionally, the isotherm onsets shifted to larger molecular areas in an almost linear way with growing molar mass of the macromonomers. Furthermore, stability experiments of our macromonomers under static and dynamic conditions revealed limited stability of the macromonomer monolayers at the air-water interface. In fact, the macromonomer films with HLB values > 8 were more stable than the hydrophobic ones with HLB < 8, which we attributed to the anchoring effect of the PEG-tail at the air-water interface. Moreover, the film degradation during hysteresis

experiments increased almost linearly with rising HLB values of the macromonomers. Based on the partial film recovery, we propose an interplay between a reversible folding and an irreversible submersion mechanism for the macromonomer monolayers at the air-water interface. As our macromonomers provide a polymerizable unit for covalent attachment, have several furan moieties, which can be used for post-synthetic Diels-Alder reactions and are able to form monolayers at the air-water interface, we believe they are promising surface functionalization reagents of hydrogels, even if the macromonomer films show limited stability. According to our surface functionality ranking, PFGE<sub>10</sub>-*b*-PEG<sub>9</sub> is the most promising hydrogel surface functionalization reagent among our macromonomers, because it can introduce the highest number of functional groups per surface area.

## Conflicts of interest

The authors declare no conflict of interest.

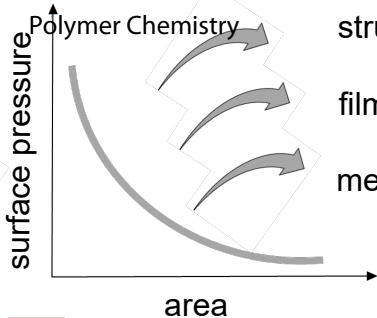
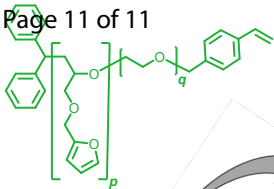
## Acknowledgements

K. A. thanks the Evonik Foundation for financial support. The authors thank the University of Stuttgart and Stanford University for provision of infrastructure. Part of this work was performed at the Stanford Nano Shared Facilities (SNSF, Stanford University), supported by the National Science Foundation under award ECCS-1542152. We gratefully acknowledge generous financial support by the Carl Zeiss Foundation and the University of Stuttgart within the *Projekthaus NanoBioMater*.

## References

1. I. Langmuir, *J. Am. Chem. Soc.*, 1917, **39**, 1848 - 1906.
2. P. Dynarowicz-Łątka, A. Dhanabalan and O. N. Oliveira Jr, *Adv. Colloid Interface Sci.*, 2001, **91**, 221-293.
3. G. C. Nutting and W. D. Harkins, *J. Am. Chem. Soc.*, 1939, **61**, 1180-1187.
4. B. Brugger, J. Vermant and W. Richtering, *Phys. Chem. Chem. Phys.*, 2010, **12**, 14573-14578.
5. K. Shimizu, J. N. Canongia Lopes and A. I. M. Gonçalves da Silva, *Langmuir*, 2015, **31**, 8371-8378.
6. A. Modlińska and D. Bauman, *Int. J. Mol. Sci.*, 2011, **12**, 4923-4945.
7. L. Komitov, B. Stebler, G. Gabrielli, M. Puggelli, A. Sparavigna and A. Strigazzi, *Mol. Cryst. Liq. Cryst. Sci. Technol.*, 1994, **243**, 107-124.
8. V. Fazio, L. Komitov and S. Lagerwall, *Thin Solid Films*, 1998, **327**, 681-685.
9. M. Faure, P. Bassereau, M. Carignano, I. Szleifer, Y. Gallot and D. Andelman, *Eur. Phys. J. B.*, 1998, **3**, 365-375.
10. J. Miñones, M. M. Conde, E. Yebra-Pimentel and J. M. Trillo, *J. Phys. Chem. C.*, 2009, **113**, 17455-17463.
11. A. Holm, L. Kunz, A. R. Riscoe, K.-C. Kao, M. Carnello and C. W. Frank, *Langmuir*, 2019, **35**, 4460-4470.
12. M. Liu, A. Kira and H. Nakahara, *Langmuir*, 1997, **13**, 779-783.

13. S.-Y. Yoo, H.-K. Shin, H. Jeong, J.-C. Park and Y.-S. Kwon, *Mol. Cryst. Liq. Cryst. Sci. Technol.*, 1999, **337**, 357-360.
14. J. T. Culp, J.-H. Park, D. Stratakis, M. W. Meisel and D. R. Talham, *J. Am. Chem. Soc.*, 2002, **124**, 10083-10090.
15. Y. Ni, R. R. Puthenkovilakom and Q. Huo, *Langmuir*, 2004, **20**, 2765-2771.
16. T. J. Joncheray, K. M. Denoncourt, C. Mathieu, M. A. Meier, U. S. Schubert and R. S. Duran, *Langmuir*, 2006, **22**, 9264-9271.
17. A. Napoli, N. Tirelli, E. Wehrli and J. A. Hubbell, *Langmuir*, 2002, **18**, 8324-8329.
18. A. Cardenas-Valera and A. Bailey, *Colloids Surf. A.*, 1993, **79**, 115-127.
19. A. Malzert, F. Boury, P. Saulnier, J. Benoit and J. Proust, *Langmuir*, 2001, **17**, 7837-7841.
20. H. d. Bijsterbosch, V. De Haan, A. De Graaf, M. Mellema, F. Leermakers, M. C. Stuart and A. v. Well, *Langmuir*, 1995, **11**, 4467-4473.
21. J. P. Kampf, C. W. Frank, E. E. Malmström and C. J. Hawker, *Langmuir*, 1999, **15**, 227-233.
22. M. C. Fauré, P. Bassereau, L. T. Lee, A. Menelle and C. Lheveder, *Macromolecules*, 1999, **32**, 8538-8550.
23. A. G. Da Silva, E. Filipe, J. d'Oliveira and J. Martinho, *Langmuir*, 1996, **12**, 6547-6553.
24. T. R. Baekmark, G. Elender, D. D. Lasic and E. Sackmann, *Langmuir*, 1995, **11**, 3975-3987.
25. M. J. Barthel, T. Rudolph, S. Crotty, F. H. Schacher and U. S. Schubert, *J. Polym. Sci., Part A: Polym. Chem.*, 2012, **50**, 4958-4965.
26. K. K. Adata, S. Keller, T. Götz, G. E. M. Tovar and A. Southan, *Polym. Chem.*, 2019, **10**, 4485-4494.
27. E. Brynda, M. Houska, J. Kysilka, M. Pěrdný, P. Lesný, P. Jendelová, J. Michálek and E. Syková, *J. Mater. Sci. Mater. Med.*, 2009, **20**, 909-915.
28. S. Sajeesh, K. Bouchemal, C. Sharma and C. Vauthier, *Eur. J. Pharm. Biopharm.*, 2010, **74**, 209-218.
29. X. Hu, H. Tan, X. Wang and P. Chen, *Colloids Surf. A.*, 2016, **489**, 297-304.
30. Y. T., W. Q., J. D. S., W. M. D. and O. C. K., *Adv. Funct. Mater.*, 2005, **15**, 1303-1309.
31. M. R. Hynd, J. P. Frampton, M.-R. Burnham, D. L. Martin, N. M. Dowell-Mesfin, J. N. Turner and W. Shain, *J. Biomed. Mater. Res. A.*, 2007, **81A**, 347-354.
32. W. C. Griffin, *J. Cosmet. Sci.*, 1949, **1**, 311-326.
33. W. C. Griffin, *J. Cosmet. Sci.*, 1954, **5**, 249-256.
34. N. Bolourchian, M. M. Mahboobian and S. Dadashzadeh, *J. Pharm. Pharm. Sci.*, 2013, **12**, 11.
35. K. N. Sill, B. Sullivan, A. Carie and J. E. Semple, *Biomacromolecules*, 2017, **18**, 1874-1884.
36. A. Dhanabalan, L. Gaffo, A. M. Barros, W. C. Moreira and O. N. Oliveira, *Langmuir*, 1999, **15**, 3944-3949.
37. A. Angelova, D. Vollhardt and R. Ionov, *J. Phys. Chem. B.*, 1996, **100**, 10710-10720.
38. C. Constantino, A. Dhanabalan and O. Oliveira Jr, *Rev. Sci. Instrum.*, 1999, **70**, 3674-3680.
39. H. Yang, K. Shin, G. Tae and S. K. Satija, *Soft matter*, 2009, **5**, 2731-2737.
40. T. Wiesenhal, T. R. Baekmark and R. Merkel, *Langmuir*, 1999, **15**, 6837-6844.
41. E. M. Clop, N. A. Corvalán and M. A. Perillo, *Colloids Surf. B.*, 2016, **148**, 640-649.
42. S. O. Kyeremateng, E. Amado, A. Blume and J. Kressler, *Macromol. Rapid Commun.*, 2008, **29**, 1140-1146.
43. L. Deschênes, F. Saint-Germain and J. Lyklema, *J. Colloid Interface Sci.*, 2015, **449**, 494-505.
44. P. Ramírez, L. M. Pérez, L. A. Trujillo, M. Ruiz, J. Muñoz and R. Miller, *Colloids Surf. A.*, 2011, **375**, 130-135.
45. A. D. McNaught and A. Wilkinson, 1997, **Blackwell Scientific Publications**, Oxford.
46. C. Barentin, P. Muller and J. F. Joanny, *Macromolecules*, 1998, **31**, 2198-2211.
47. T. E. Goto and L. Caseli, *Langmuir*, 2013, **29**, 9063-9071.
48. K. Y. C. Lee, *Annu. Rev. Phys. Chem.*, 2008, **59**, 771-791.
49. S. A. Safran and M. Schick, *Phys. Today*, 1996, **49**, 68.
50. S. Leibler, *World Scientific*, 2004, 49-101.
51. A. Gopal and K. Y. C. Lee, *J. Phys. Chem. B.*, 2001, **105**, 10348-10354.
52. C. Ybert, W. Lu, G. Möller and C. M. Knobler, *J. Phys. Chem. B.*, 2002, **106**, 2004-2008.
53. H. Diamant, T. A. Witten, C. Ege, A. Gopal and K. Y. C. Lee, *Phys. Rev. E.*, 2001, **63**, 061602.
54. T. Ivanova, I. Panaiotov, G. Georgiev, M. A. Launois-Surpas, J. E. Proust and F. Puisieux, *Colloids Surf. A.*, 1991, **60**, 263-273.
55. V. G. Levich, *Physicochemical hydrodynamics*, Prentice hall, 1962.
56. M. M. Lipp, K. Y. C. Lee, D. Y. Takamoto, J. A. Zasadzinski and A. J. Waring, *Phys. Rev. Lett.*, 1998, **81**, 1650-1653.
57. S. Baoukina, L. Monticelli, H. J. Risselada, S. J. Marrink and D. P. Tieleman, *Proc. Natl. Acad. Sci.*, 2008, **105**, 10803-10808.
58. H. E. Ries Jr and H. Swift, *Langmuir*, 1987, **3**, 853-855.
59. J. Ding, D. Y. Takamoto, A. von Nahmen, M. M. Lipp, K. Y. C. Lee, A. J. Waring and J. A. Zasadzinski, *Biophys. J.*, 2001, **80**, 2262-2272.
60. D. Y. Takamoto, M. M. Lipp, A. von Nahmen, K. Y. C. Lee, A. J. Waring and J. A. Zasadzinski, *Biophys. J.*, 2001, **81**, 153-169.
61. E. Rivera, M. del Pilar Carreón-Castro, L. Rodríguez, G. Cedillo, S. Fomine and O. G. Morales-Saavedra, *Dyes Pigm.*, 2007, **74**, 396-403.
62. R. Maget-Dana, *Biochim. Biophys. Acta*, 1999, **1462**, 109-140.
63. K. Das and S. Kundu, *Colloids Surf. A.*, 2016, **492**, 54-61.



structure-property

film stability

mechanism

air



water